Green Synthesis of Manganese Oxide Nanoparticles by Aqueous Extract of Conocarpus Erectus L. Leaves

Safaa Adil Abdulameer[1], Rihab Edan Kadhim[2]
[1], [2] Department of Biology, College of Science, University of Babylon, Hilla, Iraq.
*Corresponding other: Email: safaabiology98@yahoo.com

Abstract
The aqueous leaves extract of Conocarpus erectus L. was used to create the manganese nanoparticles, or MnONPs. When the leaf extract (5% w/v) is combined with MnCl2 (1M), the MnONPs become visible after a few hours with a color shift. Atomic force microscopy (AFM), scanning electron microscopy (SEM), X-ray diffraction (XRD), Fourier transform infrared (FTIR), and UV-S were used to analyze MnONPs. The manganese nanoparticle size, as determined by XRD, was approximately 9 nm, while the aggregate size ranged between 14 and 67 nm, depending on SEM, when employing UV-S. The use of FTIR technology revealed the existence of phenol and other chemical active sites. All of these measurements were made using MnONPs and plant extract separately for comparison.
Keywords: Conocarpus sp., Mn NPs, UV-S, XRD, FTIR, SEM, Aqueous extract.

1. Introduction

The merger of the fields of nanotechnology and biotechnology is known as nano biotechnology. According to Shahcheraghi et al. (2022), nano-based technologies are being developed to enhance conventional biotechnological methods and get over their drawbacks, like the adverse effects of conventional medicines. Studies have shown that the use of nanobiotechnology has significantly improved the effectiveness of many different procedures, including enzymatic reactions, water and soil remediation, and drug delivery. Nanotechnology is the combination of engineering, chemical, and biological methods to manipulate the material universe atom by atom. Applications of nanoscale materials and structures are a developing field of nanoscience and nanotechnology, often ranging from 1-100 nm (Jayandran et al., 2015). With several uses in energy, materials, computer chips, manufacturing, health care, and medical diagnosis, nanotechnology has emerged as a rapidly growing sector. Products generated from nanotechnology are referred to as nanomaterials... Over 800 nonmaterial products are presently thought to be on the market, and it is anticipated that this number will rise over the following few years (Aslani et al., 2014). The delivery of plant hormones, seed germination, water management, transfer of target genes, nanobarcoding, nanosensors, and controlled release of agrichemicals are currently being investigated as applications of nanotechnology in agriculture (Worrall et al., 2018). Because it is involved in photosynthesis, respiration, and the metabolism of nitrogen (N), manganese (Mn) is an essential nutrient that plants need in trace amounts. Additionally, Mn plays a role in granting pathogens that affect roots and shoots tolerance (Dimkpa et al., 2018). Understanding the interactions of manganese (Mn), which is required in minute amounts for appropriate plant growth and development, is crucial for cultivating environmentally friendly and sustainable crops. The physiological processes in plant cells are distorted by both a lack of this element and an overabundance in the environment. Despite the fact that several articles have suggested that Mn and its compounds are contaminating soil at an increasing rate, relatively little is known about Mn's harmful consequences (Sieprawska et al., 2022). In therapeutic procedures, the use of photochemical and plant extracts, both of which have proven antibacterial capabilities, can be quite important. Numerous studies have been carried out recently in a variety of nations to demonstrate this effectiveness (Nascimento et al., 2000). Conocarpus trees are attractive evergreen trees that are part of the Combretaceae family. There are around 500 species in the family and roughly 18 geniuses. Conocarpus trees are among the significant ornamental trees produced primarily for aesthetic, climatic, and recreational purposes. Due to their resistance to environmental conditions like high temperatures and salinity, they can also be grown in deserts (Halawa et al., 2019). The Conocarpus tree is used in many nations throughout the world for traditional medicine. Because it has antiplasmodial, antileishmanial, and antitrypanosomal properties, it is used as a diuretic and in the treatment of numerous illnesses, including worms, acute enteritis, colitis, constipation, tooth decay, general infections, malaria, tuberculosis, respiratory diseases, and cancer (Afifi et al., 2021). Due to the plant's secondary chemicals, some research was interested in producing nanopolines from it (Kadhim and Abd, 2018; Khadhim and Kadhim, 2021). With the aid of an extract from Conocarpus leaves, this study sought to synthesize Mn as a MnONP.

2. Materials and Methods

Leaves collection

On August 26, 2022, a collection of C. erectus L. leaves was made on the campus of Babylon University. The

doi.org/10.31838/hiv23.03.300 Received: 17.11.22, Revised: 21.12.22, Accepted: 23.01.23.

leaves are thoroughly ground, cleaned, and stored in a clean, closed container before being rinsed with deionized water, dried at room temperature, and used as needed.

Preparation of aqueous leaf extract of *C. erectus*

A mixture of 95 ml of distilled water and five grams of powdered C. erectus leaves cooked at 60 °C for 15 minutes. The mixture was next filtered using gauze paper (4 layers), and to boost purity, brown watery extract was then twice filtered using filter paper no. 1. The ensuing experiment made use of the filtrate. Synthesis of manganese nanoparticles (MnNPs) from leaves extract of C. erectus

One molar of manganese chloride was prepared using Vaishnav et al. (2017)'s modification approach. 170 ml of MnCl2 and 30 ml of C. erectus extract were combined. The mixture's hue altered after 11 hours, and a hazy substance suddenly formed. To improve sedimentation with a gradual color change from brilliant brown to dark green at pH 11–12, drops of 1M NaOH were gradually applied. After 24 hours of incubation at lab temperature, the mixture was centrifuged for 15 minutes at 6000 rpm. The precipitate (manganese nanoparticle) was obtained after drying and subjected to the following procedures, with the supernatant being discarded. X-Ray Diffractometer (Dx2700BH), UV-Vis (Model Lambda 365 Perkin Elmer)

, AFM (Atomic Force Microscopy) (Model TT-2 AFM workshop), FTIR (Fourier Transform Infrared) **(**Model Spectrum TWO Perkin Elmer), and SEM (Scanning Electron Microscopy) (inspect f50). As shown in numerous study studies (Hoseinpour & Ghaemi, 2018; Kadhim & Abd, 2018; Alrubaie and Kadhim, 2019), these methodologies are crucial to identifying the properties of MnONPs.

3. Results and Discussion

Color changes

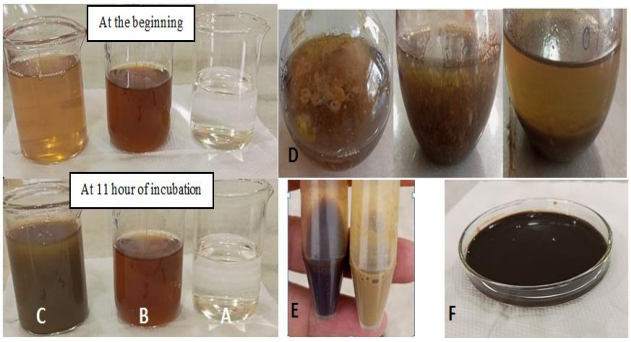

Figure 1: Color change comparing between the mixture of C. erectus extract and MnCl2 (C) at the beginning of experiment and the change in color appearance after11 hour, (A) MnCl2, and (B) C. erectus extract. (D) The graduate precipitation after NaOH (1M) adding. (E) Comparing between MnNPs before drying (dark brown) and C. erectus extract alone (light brown). (F) MnNPs for drying.

At around 11 hours, the color of the C. erectus extract and MnCl2 mixture changed from light brown to dark brown, reflecting the biological synthesis of MnONPs, which initially started as fuzzy rings before changing to irregular-shaped particles when NaOH was added. The dark brown color of the MnONPs following purification. Figure 1 illustrates how the sedimentation's appearance and color shift can be seen with the naked eye. It is abundantly obvious that the C. erectus extract caused the creation of well-reduced and stable MnONPs. For the synthesis of MnONPs, the color change varies depending on the plant species (Jayandran et al., 2015).

UV-visible Spectrum

The MnONPs (blue line) and plant extract (red line) curves both showed that their maximum absorption occurred at 190 nm, but the MnONPs were more stable between 190 and 265 nm. According to Rathi et al. (2006), this rise in absorption intensity denotes improved solubility and dispersion of the NPs in solution. The creation of MnONPs may be indicated by the absorption at wavelength 265 nm. According to Hoseinpour et al. (2018), in ideal conditions, the UV-vis absorption of MnONPs stabilized by curcumin reached the maximum absorption at 240 nm.

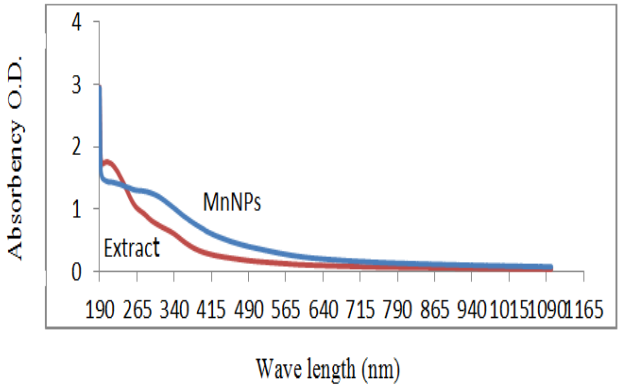

Figure 2: Absorption spectrum of synthesized MnNPs by C. erectus leaf extract

Fourier Transform Infrared (FT-IR)

Figures 3a and 3b outline the functional groups in the C. erectus leaf extract and describe how they contribute to the production of manganese oxide nanoparticles. The results of the FTIR study show the presence of bio-components on the nanoparticles' surface, which interacted with the molecules of MnCl2 and proteins to reduce Mn ions and stabilize MnO NPs. According to Muzaffar and Tahir (2018), plant components are crucial to the reduction of metal ions. To locate the relevant functional group present in the C. erectus leaves extract biomolecules that reduce the manganese ions, the FT-IR spectroscopy technique is crucial. The maxima for MnONPs and plant extract are shown in Figures 3a and 3b, respectively. The large peak at 3421 cm1 in Fig. 3a's spectra of the MnONPs corresponds to an O-H. that allude to phenol. MnO NPs were the cause of the peak about 671 cm1 (Kumar et al., 2017). The peaks at 1638 cm1, which is a prominent peak, reflect the C=O bond. The peaks around 2357, 2330, and 2078 cm1 pertain to the -CC and -CN bonds.

The aromatic C=C bond that surrounds the NPs in the plant extract and prevents NP aggregation is related to the peaks between 1558 and 1506 cm1. The peaks at 700 to 1472 cm1 were used to identify the C-O, C-N, and C-C bands in the extract of Conocarpus leaves. the extracts' FT-IR spectra (Fig. 3b) The peaks at 1500–1700 pertain to C=C bands of aromatic rings of phenolic compounds, and they also demonstrate the OH bending modes of the phenolic compounds of the extracts that are responsible for the reduction of ions. The effect of the extracts on the synthesis of the NPs is indicated by a comparison of the spectra of the extracts and MnONPs (Hoseipour et al., 2018).

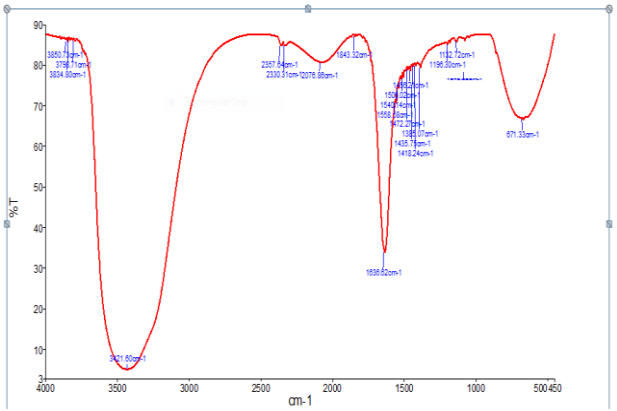

Wavenumber, cm-1

Figure 3a: FT-IR spectrum of the biosynthesized nanoparticles of MnO by Conocarpus leaves extract.

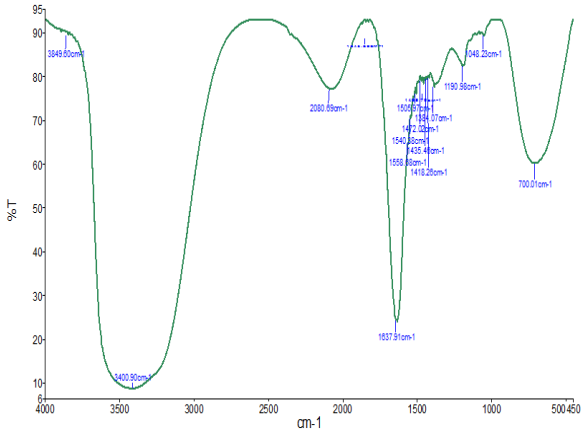

Wavenumber, cm-1

Figure 3b: FT-IR spectrum of the Conocarpus leaves extract.

X-ray Diffraction By using X-ray diffraction to analyze the crystallography of MnONPs, researchers were able to gain insight into the crystallinity of these nanoparticles. Figure (4a) shows the XRD spectra of MnONPs made from Conocarpus leaf extract. At about 2, there were numerous sharp, thin diffraction peaks that were most frequent at 18.856 °, 37.765 °, 45.428 °, and 77.789 °. According to Balamurugan et al. (2015), the produced samples were highly crystalline as evidenced by the prominent peak of the XRD. The average crystalline size of the produced MnO NPs ranges from 5 to 19 nm (fig. 4a). There was no distinct peak as compared to the extract (fig. 4b). It was observed that the diffracted intensity varied between 10° and 80° 2theta angles.

The Debye-Scherrer equation was used to compute the size of the nanoparticle, which suggests that the nanoparticle has a spherical crystal structure. D= K / cos, where D- is the particle size in nm, K is the constant is Scherrer (0.9), is the X-ray wavelength, is the full width at half maximum, and is the Bragg reflective angle. Hoseinpour et al. (2018) reported employing curcumin and yucca gloriosa leaf extract as reducing and stabilizing agents, respectively, to successfully synthesis MnO2 NPs with a size of about 80 nm.

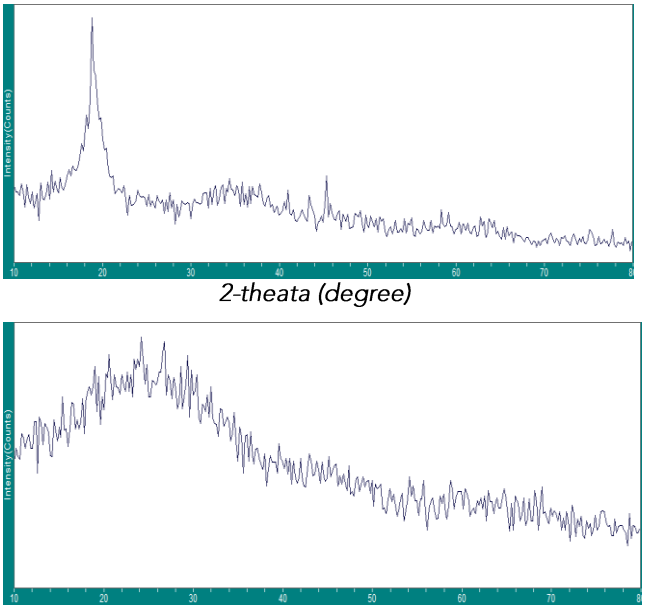

2-theata (degree)

2-theata (degree)

Figure 4: X-ray diffraction (XRD) results for MnO NPs (A) and rfor Conocarpus leaves extract (B).

Energy Dispersive X-ray Crystallography ((EDAX)

An investigation of dispersive energy X-ray crystallography (EDAX) was used to characterize the structural properties of MnO NPs.

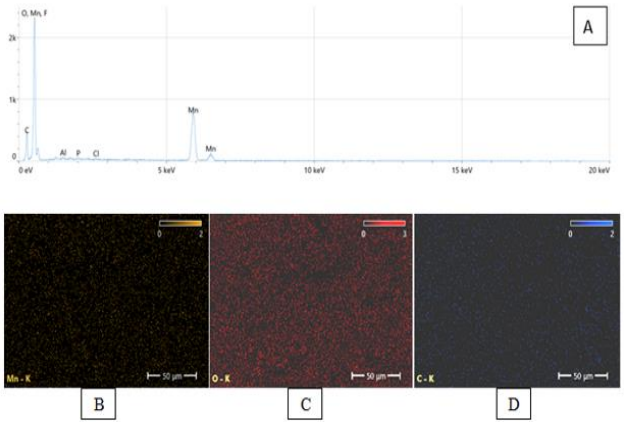

Figure 5: EDAX Spectrum showed the purity of MnO NPs. (A) Curve of EDAX. (B) Carbon (D), Manganese (C), and Oxygen.

Figure 5 illustrates how the production of MnO NPs may be involved in both quantitative and qualitative analyses. It is confirmed that biosynthesized ZnONPs include metallic zinc oxide. Three peaks were detected as manganese (49.6%), oxygen (35.5%), and carbon (10.5%) in the composition that was

obtained from the analysis of the EDAX, and there were additional peaks for aluminum, fluorine, phosphorus, and chlorine with extremely small percentages. The presence of C and O in trace levels together with the absorption peaks of higher counts for Mn shows that plant phytochemical groups are involved in the capping and reduction of produced MnO NPs (Bala et al., 2015).

Field Emission Scanning Electron

It's a technique for determining the distribution, size, and shape of manganese oxide nanoparticles that have been manufactured. Figure 6 shows several aggregates and individual MnO nanoparticles. The particles were round and ranged in size from 14 to 67 nm. To create MnONPs, it's crucial to use an extract from Conocarpus leaves as a reducing agent. According to the photos, there is secondary material capping the NPs, which was attributed to bioorganic chemicals that produced and stabilized the spherical MnONPs (Wang et al., 2007; Moon et al., 2015). The manganese oxide nanoparticles from the Conocarpus biosynthesized nanoparticle show agglomeration, which happened throughout the synthesis process, according to SEM inspection. The material's polymorphic morphology, as seen in the SEM image (fig. 6), was consistent with the findings of Jayandran et al., (2015) and Ahmed. (2020).

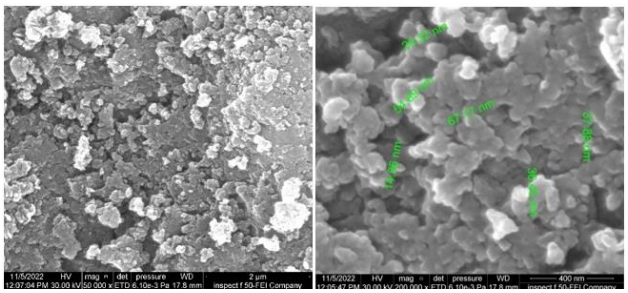

Figure 6: FESEM of MnONPs in different magnification ranges 2 and 400 µm shows size and shape of MnONPs.

Atomic force microscopy (AFM)

AFM has proven to be the ideal instrument for investigating nanoscale phenomena, including quantitative single molecule studies. The development of new medications, the development of their delivery systems based on polymers or inorganic/metallic matrices, and the analysis of disease-related tissue changes are all made possible by a variety of novel AFM techniques (Maver et al., 2016). The MnONPs and extract had different particle sizes, conical-shaped particle distributions, and overall sample roughness, according to atomic force microscope scanning (figure 7a & b). The visual representations demonstrate that MnONPs (fig.7a) had more well ordered particles than the extract sample (fig.7b). Particle sizes in the MnONPs samples were 66% smaller (512.86 253.39 nm3) than in the extract sample (1506.32 194.81 nm3), which was statistically significant (p 0.05). The difference in particle size and distribution is what causes the MnONPs sample to have less roughness (15.68 nm) than the extract sample (21.05 nm). The extract sample's maximum particle height (22 nm) was substantially greater than the nano-treated sample's (12 nm) maximum particle height.

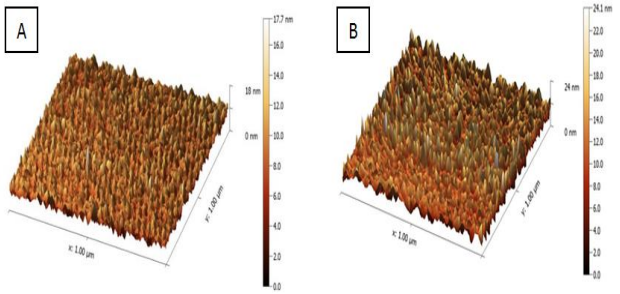

Figure 7: The image was scanned using the AFM. The scanning size was 1 µm. Scale bar represents the height of the particles in the image. A: MnONPs, B: Conocarpus leaves extract.

4. Conclusion

Conocarpus plant leaf extract was used in a green synthesis technique for MnONPs that produced MnO nanoparticles and served as a reducing agent to shrink the particles to nano size. The produced MnONPs were examined using techniques like UV-Vis spectroscopy, XRD, FTIR, FESEM, and AFM. These provide a quick and safe method for understanding the synthesis mechanism of MnO nanoparticles made from other plant extracts.

References

Afifi, H. S., Al Marzooqi, H. M., Tabbaa, M. J., & Arran, A. A. (2021). Phytochemicals of Conocarpus spp. as a natural and safe source of phenolic compounds and antioxidants. Molecules, 26(4), 1069.

Ahmed, M.U.; Dahiru, J.N.; Sudi, I. Y. Gabriel, S. and John, I. K. (2020). Green Synthesis of Manganese Oxide Nanoparticles from Cassia tora Leaves and its Toxicological Evaluation, Asian J. Applied Sci., 13 (2): 60-67.

Alrubaie, E. A. A. A., & Kadhim, R. E. (2019). Synthesis of ZnO nanoparticles from olive plant extract. Plant Archives, 19(2), 339-344.

Aslani, F., Bagheri, S., Muhd Julkapli, N., Juraimi, A. S., Hashemi, F. S. G., & Baghdadi, A. (2014). Effects of engineered nanomaterials on plants growth: an overview. The Scientific World Journal, 1-28.

Bala, N.; Saha, S.; Chakraborty, M.; Maiti, M.; Das, S;. Basu, R. and Nandy, P. (2015). Green synthesis of zinc oxide nanoparticles using *Hibiscus subdariffa* leaf extract effect of temperature on synthesis, anti-bacterial activity and anti-diabetic activity, RSC Adv., 5: 4993–5003.

Balamurugan, M.; Venkatesan, G; Ramachandran, S. and Saravanan, S. (2015). Synthesis and Characterization of Manganese Oxide Nanoparticles Synthesis and Fabrication of Nanomaterials, 311-314.

Dimkpa, C. O., Singh, U., Adisa, I. O., Bindraban, P. S., Elmer, W. H., Gardea-Torresdey, J. L., & White, J. C. (2018). Effects of manganese nanoparticle exposure on nutrient acquisition in wheat (*Triticum aestivum* L.). Agronomy, 8(9), 158

Halawa, A. E., Zedan, A. F., & Al-Sherbini, A. S. A. (2019). Management of Soil-borne Fungal Diseases

of *Conocarpus erectus* transplants using silver nanoparticles. Sciences, 9(03), 686-699.
Hoseinpour, V. & Ghaemi, N. (2018). Green synthesis of manganese nanoparticles: Applications and future perspective–A review. Journal of Photochemistry and Photobiology B: Biology, 189: 234-243.
Hoseinpour,V.; Mahsa Souri, Nasser Ghaemi. (2018). Green synthesis, characterisation, and photocatalytic activity of manganese dioxide nanoparticles. Micro & Nano Letters, 13(11):1560–1563.
Jayandran, M., Haneefa, M. M., & Balasubramanian, V. (2015). Green synthesis and characterization of Manganese nanoparticles using natural plant extracts and its evaluation of antimicrobial activity. Journal of Applied Pharmaceutical Science, 5(12), 105-110.
Kadhim, R. E. and Abd, S. Y. (2018). Synthesis of Copper Nanoparticles Biologically by *Conocarpus erectus* L. Aqueous Leaves Extract. Journal of University of Babylon, Pure and Applied Sciences, 26 (5): 95-102.
Khadhim, A. I. and Kadhim, R. E. (2021). Synthesis of Cobalt Nanoparticles Biologically by Conocarpus erectus L. Aqueous Leaves Extract. Annals of R.S.C.B., 25 (3): 5361 – 5372.
Maver, U.; Tomaž V.; Miran G.; Odon P. and Matjaž F. (2016). Recent progressive use of atomic force microscopy in biomedical applications. Trends in Analytical Chemistry, 80: 96-111.
Moon, S.A., Salunke, B.K., Alkotaini, B., et al.(2015) Biological synthesis of manganese dioxide nanoparticles by Kalopanax pictus plant extract', IET Nanobiotechnol., 9, (4): 220–225.
Muzaffar, S., Tahir, H. (2018). Enhanced synthesis of silver nanoparticles by combination of plants extract and starch for the removal of cationic dye from simulated waste water using response surface methodology, J.Mol. Liq., 252: 368–382.
Nascimento, G. G., Locatelli, J., Freitas, P. C., & Silva, G. L. (2000). Antibacterial activity of plant extracts and phytochemicals on antibiotic-resistant bacteria. Brazilian journal of microbiology, 31, 247-256.
Rathi, B., Bodhankar, S., Baheti, A. (2006). Evaluation of aqueous leaves extract of Moringa oleifera Linn for wound healing in albino rats.
Savelev, S.U., Okello, E.J., Perry, E.K.: (2004). Butyryl- and acetyl-cholinesterase inhibitory activities in essential oils of salvia species and their constituents. Phytother. Res., 18, (4): 315–324.
Shahcheraghi, N; Hasti, G.;Zahra, S.; Yasaman, T.;Forough, B. and Shadi, M. (2022). Nano-biotechnology, an applicable approach for sustainable future, 3 Biotech., 12(65).
Sieprawska, A., Rudolphi-Szydło, E., Barbasz, A., Skórka, M., Telk, A., & Filek, M. (2022). Biochemical estimation of manganese nanoparticles reactions in native and model biological systems.
Vaishnav, J.; subha, V.; Kirubanandan, S.; Arulmozhi, M. and and Renganathana, S. (2017). Green synthesis of zinc oxide nanoparticles by *celosia Argentea* and its characterization. India Journal of Optoelectronics and Biomedical Materials., 9(1) : 562–566.
Wang, M., Na, E.K., Kim, J.S., et al. (2007). Photoluminescence of ZnO nanoparticles prepared by a low-temperature colloidal chemistry method. Mater. Lett., 61(19): 4094–4096.
Worrall, E. A., Hamid, A., Mody, K. T., Mitter, N., & Pappu, H. R. (2018). Nanotechnology for plant disease management. Agronomy, 8(12), 285.